Online continuous-time adaptive predictive control of the technological glass conditioning process

Michał DRAPAŁA and Witold BYRSKI

Glass production has a great industrial importance and is associated with many technological challenges. Control related problems concern especially the last part of the process, so called glass conditioning. Molten glass is gradually cooled down in a long ceramic channels called forehearths during glass conditioning. The glass temperature in each zone of the forehearth should be precisely adjusted according to the assumed profile. Due to cross-couplings and unmeasured disturbances, traditional control systems based on PID controllers, often do not ensure sufficient control quality. This problem is the main motivation for the research presented in the paper. A Model Predictive Control algorithm is proposed for the analysed process. It is assumed the dynamic model for each zone of the forehearth is identified on-line with the Modulating Functions Method. These continuous-time linear models are subsequently used for two purposes: for the predictive controller tuning, measurable disturbances compensation and for a static set point optimisation. Proposed approach was tested using Partial Differential Equation model to simulate two adjacent zones of the forehearth. The experimental results proved that it can be successfully applied for the aforementioned model.

Key words: system identification, modulating functions method, model predictive control, continuous-time systems, glass forehearth

1. Introduction

Continuous technological processes with uninterrupted operation and significant energy consumption pay particular attention among other processes. Such processes are typical for chemical and petroleum rectification, metallurgical and glass industries. Distillation columns run continuously for a period of a year,

M. Drapała (corresponding author, e-mail: mcad111@interia.pl) and W. Byrski (e-mail: wby@agh.edu.pl) are with Department of Automatic Control and Robotics, AGH University of Science and Technology, Al. Mickiewicza 30, 30-059 Kraków, Poland

consuming energy from superheated steam, and only then there is a service break. Usually glass furnaces consume large amount of natural gas as its energy source. Typical campaign time for a glass furnace lasts about 10 years. Saving even 1% of the energy consumed throughout this time would bring significant profits for the factory and would reduce CO_2 emission substantially. Apart from production technologists, the contribution to this energy optimization problem is made by modern computer control systems, that utilize process models. Control algorithms can optimize several conflicting goals, like maximizing production, reducing energy consumption, minimizing wastes, while meeting technological constraints at the same time. In this paper, that is devoted to the process of glass containers production, a special new Adaptive Predictive Control approach will be presented, for the problems of molten glass temperature stabilization and static operating point optimization. For this purpose, new non-standard methods of continuous-time linear models identification and exact state observation will be applied.

Conditioning is a vital part of a glass manufacturing process. After leaving a glass furnace, molten glass is gradually cooled down in working end and forehearth zones, before forming containers. The purpose of this procedure is to obtain the utmost glass homogeneity in the last part of the forehearth. This parameter depends on the temperature difference between adjacent glass streams. From a technological point of view, the temperature stabilization problem at the forehearth exit is crucial for the quality of manufactured products. Equally important issue concerns the set point tracking during production changes. Fast adaptation to new working conditions allows minimizing production downtimes and saving energy.

Described problem is significant for the glass industry, however, there are little subject literature. Research works often concern the area of predictive control, e.g. in [1] the synthesis of an adaptive Generalized Predictive Control (GPC) algorithm with feedforward for the container manufacturing process is discussed. The authors claimed that the production quality was significantly improved. Similar idea for continuous models is presented in [2]. Authors of [3] and [4] developed two degree of freedom control structure composed of feedforward and feedback parts for forehearth zone described with Partial Differential Equation (PDE) model. Another approach utilizes the concept of Computational Fluid Dynamics (CFD) simulation. It is described in [5] and [6]. The solution implements predictive control algorithms. Additional features enable to consider dependencies between technological parameters and to optimize working conditions for the whole glass melting plant. Detailed description of the identification and control algorithms is omitted due to the fact that the expert system is a commercial solution.

The research presented in this paper proposes different approach. Dynamical models of the forehearth zones are obtained by on-line identification algorithm

based on the Modulating Functions Method (MFM). Standard methods of active identification based on step response apply only to low-order linear continuous systems with zero initial conditions. Passive identification of continuous (not discrete) linear systems of any order is not trivial and searching for an efficient method of such identification is important for control theory. The linear models are identified for successive time intervals. With a change of operating conditions, parameters of these models can be updated. The models are utilized to tune the Model Predictive Controller (MPC) and to optimize the current operating point. The paper summarizes and expands previously described adaptive identification approach described in [7] and [8], as well as the continues-time model predictive algorithm presented in [9]. The algorithm of temperature set-point optimization is the novelty introduced in the work.

The paper is organized as follows. Section 2 gives a short description of the analyzed glass forehearth installation and its control system. Section 3 presents in details the implemented on-line identification algorithm based on the MFM. Developed control methods are explained in Section 4. Section 5 reports the experimental results. The last Section 6 concludes the paper.

2. Forehearth control system

The glass production process can be divided into several steps:

- melting batch materials,

- clarification,

- homogenization,

- rafination,

- conditioning.

The first three stages take place in a glass furnace, while the last two of them are performed after molten glass leaves the furnace, in other parts of the installation (working end and forehearths). During the conditioning process, the temperature difference between glass fractions is compensated. The glass acquires appropriate viscosity and temperature before forming.

As is mentioned above, the molten glass flows from the furnace into the working end. It connects the furnace with the forehearths. Each forehearth constitutes a separate production line. It is a long ceramic channel, usually divided into several zones. For the analyzed glass forehearth, each zone has its own temperature controller. The type of installed actuators depends on its role and location. The molten glass temperature should be maximally reduced in the first zone. That is

why cooling dampers are mounted here. In the second zone, there are separate gas burners for left and right sides to equalize the temperatures of the molten glass streams. The precise temperature control is especially important for the last two zones which makes reasonably to replace PID controllers by predictive ones. The control loops creating the analyzed forehearth control system are depicted in Figure 1.
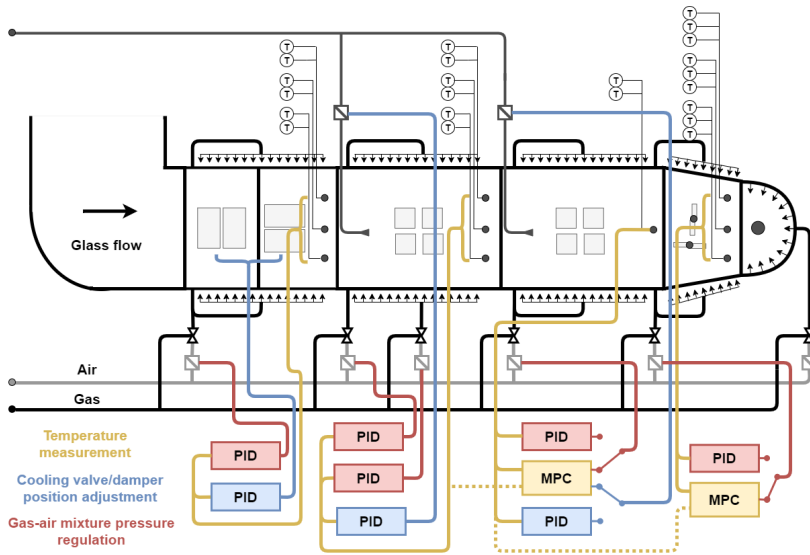

Figure 1: Control system of a glass forehearth

The amount of glass flowing through the forehearth is called a glass pull rate. This parameter is typically given in tons and defined for 24 hours. It can be reliably determined only for steady states of the installation. When operating points are changed, this parameter can vary significantly and its value is provided by operators with some delay. Its knowledge is important, because it determines the delay with which the preceding zone temperature affects the measured one.

3. Model identification algorithm

It is assumed that the Linear Time Invariant (LTI) Multi Input Single Output (MISO) system is given by Equation (1):

$$\sum_{i=0}^{n} a_i y^{(i)}(t) = \sum_{k=1}^{K} \sum_{j=0}^{m_k} b_{kj} u_k^{(j)}(t) = \sum_{j=0}^{m_1} b_{1j} u_1^{(j)}(t) + \ldots + \sum_{j=0}^{m_K} b_{Kj} u_K^{(j)}(t). \quad (1)$$

The model has single output y and K inputs u_k, where $k = 1, \ldots, K$. There are n output derivatives and m_k derivatives for the k-th input, where $m_k \leqslant n$. The functions $y^{(i)}, u_1^{(j)}, \ldots, u_K^{(j)}$ are given on the interval $[t_0, T_{ID}]$. It is assumed that only the inputs u and the output y are measured. Their derivatives can be calculated numerically, however it often results in large errors. The values of parameters $\boldsymbol{a}$ and $\boldsymbol{b}$ are not known and should be identified.

3.1. Modulating Functions Method

The identification procedure can be performed using the Modulating Functions Method (MFM) approach developed by Shinbrot [10]. It is based on the rule of integrating by parts. A comprehensive description of the method can be found in [11], as well as in [12]. It will be shortly presented below. Left and right hand sides of Equation (1) are convoluted with the filtering function ϕ and its known derivatives $\phi^{(i)}$. The function ϕ is non-zero in the interval $(0, h)$ and zero for $t = 0$, $t = h$ and outside this interval.

Utilizing the convolution properties, new functions $y_i(t)$ and $u_i(t)$ can be obtained in the interval $[t_0 + h, T_{ID}]$ for $i = 0, 1, \ldots, n$:

$$a_i y_i(t) = a_i \int_{-\infty}^{\infty} y^{(i)}(\tau)\phi(t - \tau)\,\mathrm{d}\tau = a_i \int_0^h y(t - \tau)\phi^{(i)}(\tau)\,\mathrm{d}\tau = a_i y_i(t), \qquad (2)$$

$$b_j u_{kj}(t) = b_j \int_{-\infty}^{\infty} u_k^{(j)}(\tau)\phi(t - \tau)\,\mathrm{d}\tau = b_j \int_0^h u_k(t - \tau)\phi^{(j)}(\tau)\,\mathrm{d}\tau = b_j u_{kj}(t). \quad (3)$$

Hence, the differential Equation (1) can be transformed into the algebraic Equation (4) with the same parameters:

$$\sum_{i=0}^{n} a_i y_i(t) = \sum_{j=0}^{m_1} b_{1j} u_{1j}(t) + \ldots + \sum_{j=0}^{m_K} b_{Kj} u_{Kj}(t) + \epsilon(t). \qquad (4)$$

The term ϵ represents difference between left and right-hand side terms resulting from e.g. inaccuracies arising during computations or signal noises.

For identification purposes, the following assumptions about the ϕ function were made:

- $\phi \in C^n(0, h)$ and satisfies boundary conditions $\phi^{(i)}(0) = \phi^{(i)}(h) = 0$ for $i = 0, 1, \ldots, n - 1$,

- $y * \phi = 0 \Rightarrow y = 0$ on the interval $[t_0 + h, T_{ID}]$,

- the function support h has to be less than $T_{ID} - t_0$, then Equation (4) is valid for $t \in (t_0 + h, T_{ID})$.

In the paper, the Loeb and Cahen functions were used:

$$\phi(t) = t^N(h - t)^M, \quad N < M. \tag{5}$$

The aforementioned error ϵ can be treated as a performance index of the Equation Error Method (EEM). It can be written as:

$$\epsilon(t) = c^T(t)\theta = \big[y_0(t), \ldots, y_n(t), -u_{10}(t), \ldots,$$

$$- u_{1m_1}(t), \ldots, -u_{K0}(t), \ldots, -u_{Km_K}(t)\big]
\begin{bmatrix} a \\ b_1 \\ \vdots \\ b_K \end{bmatrix}, \tag{6}$$

where a, b_1, $\ldots$, b_K are the column vectors of input and output parameters. The number of elements of the vector θ depends on the assumed rank of the identified system: $\theta \in R^{n+m_1+\ldots+m_K+K+1}$.

In [11], as well as in [12], an original approach of finding the optimal vector of parameters is described. The minimization problem is stated in the function space $L^2[t_0 + h, T_{\text{ID}}]$ as:

$$\min_{\theta} J^2 = \min \|\epsilon(t)\|_{L^2[t_0+h,T]}^2 = \min \|c(t)^T\theta\|_{L^2}^2. \tag{7}$$

The trivial solution can be avoided by introducing the linear constraint $\eta^T\theta = 1$. The norm in Equation (7) can be interpreted as an inner product in the space L^2:

$$J^2 = \langle c^T(t)\theta, c^T(t)\theta \rangle_{L^2} = \theta^T \langle c(t), c^T(t) \rangle \theta = \theta^T G\theta. \tag{8}$$

The square real and symmetric Gram matrix G is given as:

$$G = \begin{bmatrix}
YY & YU_1 & \ldots & YU_K \\
U_1Y & U_1U_1 & \ldots & U_1U_K \\
\vdots & \vdots & \ddots & \vdots \\
U_KY & U_KU_1 & \ldots & U_KU_K
\end{bmatrix}, \tag{9}$$

where:
$YY(i, j) = \langle y_i, y_j \rangle$ and $i = 0 \ldots n$, $j = 0 \ldots n$,
$YU_k(i, j) = -\langle y_i, u_{kj} \rangle$ and $k = 1 \ldots K$, $i = 0 \ldots n$, $j = 0 \ldots m_k$,
$U_kY(i, j) = -\langle u_{ki}, y_j \rangle$ and $k = 1 \ldots K$, $i = 0 \ldots m_k$, $j = 0 \ldots n$,
$U_kU_l(i, j) = \langle u_{ki}, u_{lj} \rangle$ and $k = 1 \ldots K$, $l = 1 \ldots K$, $i = 0 \ldots m_k$, $j = 0 \ldots m_l$.

The matrix G is created by the inner products in L^2 of the $c(t)$ elements, e.g.:

$$\langle y_i, u_j \rangle = \int_{t_0+h}^{T_{\text{ID}}} y_i(\tau)u_j(\tau)d\tau.$$

The optimal vector $\boldsymbol{\theta}$, that minimizes the performance index, can be calculated using the Lagrange multiplier technique:

$$\min_{\boldsymbol{\theta}} J^2 = \min_{\boldsymbol{\theta}} L = \min_{\boldsymbol{\theta}} \left(\boldsymbol{\theta}^T \boldsymbol{G} \boldsymbol{\theta} + \lambda \left[\boldsymbol{\eta}^T \boldsymbol{\theta} - 1 \right] \right), \tag{10}$$

as:

$$\boldsymbol{\theta}^0 = \frac{\boldsymbol{G}^{-1} \boldsymbol{\eta}}{\boldsymbol{\eta}^T \boldsymbol{G}^{-1} \boldsymbol{\eta}}. \tag{11}$$

The matrix $\boldsymbol{G}$ is symmetric and its eigenvalues are real and positive. In practice, it cannot be non-singular due to uncorrelated noises in signals. Having the matrix $\boldsymbol{G}$, it is possible to select the optimal constraint vector $\boldsymbol{\eta}$ that minimizes the performance index J^2. In [12] it is explained that it should be selected as the eigenvector of the matrix $\boldsymbol{G}$ corresponding to its minimal eigenvalue. However, in practical applications, when the structure of the model to be identified is unknown, it may occur that despite minimizing the value of J^2, obtained models do not give expected results. In the performed experiments the constraint vector with 1 for the n-th element and zeros for the other elements was adopted. It means that most important is obtaining the proper value of the selected parameter corresponding to the highest derivative of the output signal.

The presented MFM has many advantages among other well known identification methods. It enables to obtain continuous-time LTI models directly, without discretization. Its most important feature is the possibility to identify the models without the knowledge of their initial condition. It is possible thanks to the properly selected modulating function that zeros at the modulating interval boundaries.

3.2. State-space representation of the model

Non-linearity of the analyzed system causes changes of parameters and model structure. State-space representation is convenient for simulating of the system output with non-zero initial conditions during the adaptive identification procedure and is also used by the predictive control algorithm. The differential state equations are given as:

$$\dot{x}(t) = \boldsymbol{A}_{\mathrm{m}} x_{\mathrm{m}}(t) + \underbrace{\begin{bmatrix} \boldsymbol{B}_{\mathrm{md}} & \boldsymbol{B}_{\mathrm{mu}} \end{bmatrix}}_{\boldsymbol{B}_{\mathrm{m}}} \underbrace{\begin{bmatrix} \omega(t) \\ u(t) \end{bmatrix}}_{u_{\mathrm{m}}}, \qquad x_{\mathrm{m}}(t_0) = x_{\mathrm{m0}}, \tag{12}$$

$$y(t) = \boldsymbol{C}_{\mathrm{m}} x_{\mathrm{m}}(t),$$

where:

$$\forall t \geqslant t_0 : x_{\mathrm{m}}(t) \in R^n, \omega(t) \in R, u(t) \in R^{K-1}, y(t) \in R,$$

and the corresponding real matrices A_m, B_{md}, B_{mu}, C_m consist of parameters a_i, b_i from Equation (1) or Equation (4):

$$A_m = \begin{bmatrix} 0 & \dots & 0 & -\dfrac{a_0}{a_n} \\ 1 & \ddots & \vdots & \vdots \\ \vdots & \ddots & 0 & -\dfrac{a_{n-2}}{a_n} \\ 0 & \dots & 1 & -\dfrac{a_{n-1}}{a_n} \end{bmatrix}_{(n \times n)}, \qquad B_{md} = \begin{bmatrix} \dfrac{b_{10}}{a_n} \\ \vdots \\ \dfrac{b_{1n-1}}{a_n} \end{bmatrix}_{(n \times 1)},$$

$$B_{mu} = \begin{bmatrix} \dfrac{b_{20}}{a_n} & \dots & \dfrac{b_{K0}}{a_n} \\ \vdots & \vdots & \vdots \\ \dfrac{b_{2n-1}}{a_n} & \dots & \dfrac{b_{Kn-1}}{a_n} \end{bmatrix}_{(n \times K-1)}, \quad C_m = \begin{bmatrix} 0 & \dots & 1 \end{bmatrix}_{(1 \times n)}. \tag{13}$$

In Equation (12), the input signals are divided into two categories. The first input refers to the known disturbance signal $\omega(t) = u_{m1}(t)$. The remaining signals $u(t) = [u_{m2}(t) \dots u_{mK}(t)]^T$ can be both measured and changed. This assumption results from the specific of the the analyzed system. Molten glass temperature in the controlled zone of the forehearth is influenced control signals, like e.g. gas-air mixture pressure, and by uncontrolled impacts, like glass temperature in the preceding part of the installation.

3.3. Exact integral state observers

In the above section, it is mentioned that the simulation ability of the system dynamics with non-zero initial conditions is crucial for the developed identification algorithm. The state vector $x_m(t)$ cannot be obtained directly. It can be, however, calculated based on the measured system output $y(t)$ and the known system input $u_m(t)$.

In the paper, the exact state observers are applied. They have the structure of two integrals and can exactly reconstruct the state of the linear system. The integral observers, described in [13], guarantee obtaining the real value of the observed state for the observation interval T_{OB}. The observers are used for obtaining both initial and final state of the system. The formula for the initial system state, assuming $t_0 = 0$, is given as:

$$x_m(0) = \int\limits_0^{T_{OB}} \overline{G_1}(t) y(t) \, dt + \int\limits_0^{T_{OB}} \overline{G_2}(t) u_m(t) \, dt, \tag{14}$$

where:

$$M_0 = \int_0^{T_{OB}} e^{A_m^T \tau} C_m^T C_m e^{A_m \tau} \, d\tau,$$

$$\overline{G_1}(t) = M_0^{-1} e^{A_m^T t} C_m^T,$$

$$\overline{G_2}(t) = M_0^{-1} \left[\int_t^{T_{OB}} e^{A_m^T \tau} C_m^T C_m e^{A_m \tau} \, d\tau \right] e^{-A_m t} B_m.$$

On the other hand, the final state observer is given as:

$$x_m(T_{OB}) = \int_0^{T_{OB}} G_1(t) y(t) \, dt + \int_0^{T_{OB}} G_2(t) u_m(t) \, dt, \tag{15}$$

where:

$$G_1(t) = e^{A_m T_{OB}} M_0^{-1} e^{A_m^T t} C_m^T,$$

$$G_2(t) = e^{A_m T_{OB}} M_0^{-1} \left[\int_0^t e^{A_m^T \tau} C_m^T C_m e^{A_m \tau} \, d\tau \right] e^{-A_m t} B_m.$$

3.4. Adaptive identification method

The identification method concept bases on the non-linear system dynamics described by the linear model close to the selected operating point with the use of the previously registered system inputs and outputs. The procedure is therefore analogous to the Prediction Error Method (PEM). The whole identification window is divided into smaller intervals of the width T. The subsequent zero points t_{0j} can be defined in the intervals, where input and output signals are almost constant.

The initial model of the process, valid for the zero point t_{01}, can be identified for n_{start} intervals, assuming a zero initial condition. The MFM identification procedure is performed for several predefined model sets, differing in structure and parameters values. The model with the minimal value of the performance index:

$$E(t_0, t_{end}) = \int_{t_0}^{t_{end}} (y(t) - y_{sim}(t))^2 \, dt, \tag{16}$$

where $y(t)$ is the real system output and $y_{sim}(t)$ the simulated one, is selected as a current model. Performed experiments proved that the squared difference works

better than the performance index given as Equation (8) for this task, however needs greater computational effort. To ensure reliability of the newly identified model, the historical data used for identification, should reflect significant changes of the process variables. For this reason, it is assumed that two conditions have to be met for at least two of the system inputs. First of all, the correlation between the system input and its output should be greater than tr_{corr}. Additionally, the input signals variance should be greater than tr_{var}.

Based on the identified model and the assumed input signals, the system output in the next time interval can be predicted. For this purpose, the system state for the end of the current interval t_j is needed. It can be calculated with the final state observer as:

$$x_{\text{m}}(t_j) = \int_{t_j - T_{\text{OB}}}^{t_j} \boldsymbol{G}_1(T_{\text{OB}} - t_j + t)y(t)\,\mathrm{d}t + \int_{t_j - T_{\text{OB}}}^{t_j} \boldsymbol{G}_2(T_{\text{OB}} - t_j + t)u_{\text{m}}(t)\,\mathrm{d}t, \quad (17)$$

where the successive time moments are:

$$t_j = t_{0j} + j \cdot T - (t_{0j} \quad \text{modulo} \quad T), \quad j = 1, 2, 3, \ldots$$

and t_{0j} is the current operating point.

Parameters of the current model can be updated (without changing the current operating point or the model structure) assuming that the performance index E for the current model is greater than tr_{reident}. As more process data become available, it is possible to get more reliable parameters values. The maximum re-identification interval width is equal to $n_{\text{reident}} \cdot T$.

If the new operating point can be found inside the last n_{nident} intervals, then the whole identification procedure can be performed as in the case of the first model. The condition for the model update ($E > tr_{\text{reident}}$), as well as additional conditions as for the initial model have to be met. Shorter identification window (n_{nident} base intervals instead of n_{start}) is the only difference compared with the previous procedure. If the performance index E value is less for the new model, its structure, current operating point and parameters are updated. Performing the model output simulation for this case demands applying the initial state observer (14). The above described parameters of the adaptive identification method, that were used during the performed experiments, are compiled in Table 1. Their values were selected arbitrarily on the basis of performed experiments.

It should be mentioned here that the MFM does not require zero initial conditions, which is a significant advantage of this approach. The state observers are used in the developed method only for simulating the system output in order to determine the performance index (16) value. The described approach, based on linear models identified on-line, was succesfully used for the problem of glass conditioning process modeling. The results can be found in [7] and [8].

Table 1: Parameters of the identification procedure

Parameter	Value
T	250 s
T_{OB}	500 s
tr_{var}	$1 \cdot 10^{-2}$
tr_{corr}	$5 \cdot 10^{-1}$
$tr_{reident}$	500
n_{start}	8
$n_{reident}$	16
n_{nident}	4

4. Control algorithm design

Model Predictive Control (MPC) is one of the most important concepts of Advanced Control Methods [14]. It is widely used in process industries, but mainly in so-called big industries like chemical or petrochemical [15]. In case of smaller industrial plants, traditional PID control loops are widely used. The main aim of the paper is to propose their replacement by predictive controllers for the glass conditioning process. The predictive control could solve many difficulties specific for the analyzed process. First of all, glass temperature overshoots can be significantly reduced. Moreover, the impact of glass temperature in the preceding forehearth zone can be easily compensated . However, this approach is rarely implemented in industrial plants mainly due to the difficulties with obtaining the process model.

Unlike most common approaches, utilizing discrete-time process models, as it is pointed out in [16], the described algorithm is based on the described above continuous-time linear state-space representation of the process dynamics. The predictive control algorithm is based on the idea described in [17]. In this paper, the original approach is extended by taking into account a measured disturbance signal during the controller synthesis. Similar to the case of adaptive identification algorithm, the described methodology was used to control the analyzed process [9].

4.1. Continuous-time MPC algorithm with compensation of measurable disturbances

It is assumed that the system dynamics is described by Equation (12). The augmented state vector takes the following form:

$$x(t) = \begin{bmatrix} z(t)^T & y(t) \end{bmatrix}^T, \tag{18}$$

where: $z(t) = \dot{x}_{\mathrm{m}}(t)$. The state-space representation of the augmented model is given as:

$$\underbrace{\begin{bmatrix} \dot{z}(t) \\ \dot{y}(t) \end{bmatrix}}_{\dot{x}(t)} = \underbrace{\begin{bmatrix} A_{\mathrm{m}} & 0 \\ C_{\mathrm{m}} & 0 \end{bmatrix}}_{A} \underbrace{\begin{bmatrix} z(t) \\ y(t) \end{bmatrix}}_{x(t)} + \underbrace{\begin{bmatrix} B_{\mathrm{mu}} \\ 0_{1 \times K-1} \end{bmatrix}}_{B} \dot{u}(t) + \underbrace{\begin{bmatrix} B_{\mathrm{md}} \\ 0 \end{bmatrix}}_{B_{\mathrm{d}}} \dot{\omega}(t), \qquad (19)$$

$$y(t) = \underbrace{[0_{1 \times n} \quad 1]}_{C} \begin{bmatrix} z(t) \\ y(t) \end{bmatrix}.$$

Note that the original state-space Equations (12) are differentiated. In the described approach, the predicted control trajectory is modelled with the set of orthonormal Laguerre functions and its integral squared value should be bounded to ensure the estimate convergence. For this reason, the control signal derivative is approximated instead of its original trajectory. The Laguerre functions can be easily written as a matrix equation:

$$L(\tau) = \begin{bmatrix} l_1(\tau) \\ \vdots \\ l_N(\tau) \end{bmatrix} = e^{A_p \tau} L(0), \qquad (20)$$

where:

$$A_p = \begin{bmatrix} -p & 0 & \dots & 0 \\ -2p & -p & \dots & 0 \\ \vdots & \ddots & \ddots & \vdots \\ -2p & \dots & -2p & -p \end{bmatrix},$$

$$L(0) = \sqrt{2p}[1 \ \dots \ 1]^T_{(N \times 1)}.$$

The parameter p is selected arbitrarily. It is assumed that each control signal derivative is approximated with the use of N Laguerre functions. Similarly to [17], it is adopted that the future control signal derivative is calculated for the time interval $[0, \tau]$, not for $[t_i, t_i + \tau]$, where t_i is the current time moment. This assumption can be less intuitive, but thanks to this, it is clear that the matrices η and η_{d} in further equations, can be obtained once for the current model of the system.

The predicted system state at the future time $t_i + \tau$, assuming the current time t_i, is given as:

$$x(t_i + \tau | t_i) = e^{A\tau} x(t_i) + \int_0^\tau e^{A(\tau-\gamma)} B\dot{u}(\gamma)\,d\gamma + \int_0^\tau e^{A(\tau-\gamma)} B_d\dot{\omega}(\gamma)\,d\gamma. \quad (21)$$

The vector $\dot{u}(\tau)$ has $K - 1$ elements, where the k-th element for $k = 2, \ldots, K$ takes the form:

$$\dot{u}_k(\tau) \approx \sum_{i=1}^N c_{k_i} l_i(\tau) \approx L(\tau)^T \eta_k,$$

where:

$$\eta_k = [c_{k_1} \ \ldots \ c_{k_N}]^T.$$

The term $\dot{\omega}(\tau)$ can be written analogously. Equation (21) can also be written as:

$$x(t_i + \tau | t_i) = e^{A\tau} x(t_i) + \phi(\tau)^T \eta + \phi_d(\tau)^T \eta_d, \quad (22)$$

where: B_k are column vectors of B corresponding to the suitable elements of u_m and

$$\phi(\tau)^T = \int_0^\tau e^{A(\tau-\gamma)} \left[B_2 L(\gamma)^T \ \ldots \ B_K L(\gamma)^T \right] d\gamma, \quad (23)$$

$$\phi_d(\tau)^T = \int_0^\tau e^{A(\tau-\gamma)} B_d L(\gamma)^T d\gamma. \quad (24)$$

The terms ϕ and ϕ_d depend on the calculated control signal and measured disturbances accordingly.

The performance index P, given as (25), depends on the state value and the control signal within the optimization window $[0, T_p]$:

$$P = \int_0^{T_p} (x(t_i + \tau)^T Q x(t_i + \tau) + \dot{u}(\tau)^T R \dot{u}(\tau))\,d\tau = \int_0^{T_p} (e^{A\tau} x(t_i) + \phi(\tau)^T \eta$$

$$+ \phi_d(\tau)^T \eta_d)^T Q(e^{A\tau} x(t_i) + \phi(\tau)^T \eta + \phi_d(\tau)^T \eta_d)\,d\tau + \eta^T R_L \eta, \quad (25)$$

where: weighting matrices $Q \geqslant 0$, $R \geqslant 0$, the diagonal block matrix R_L is composed of K blocks, each of size $N \times N$, with values corresponding to penalties

for the control signals increments. It was assumed that the weighting matrices have the following forms:

$$Q = C^T C, \qquad R = I_K .$$

After substituting Equations (23) and (24) into Equation (25), the performance index P can be written as:

$$P = \eta^T \Omega \eta + 2\eta^T \Psi x(t_i) + x(t_i)^T \left[\int_0^{T_p} e^{A^T \tau} Q e^{A\tau} \, d\tau \right] x(t_i)$$

$$+ \eta_d^T \left[\int_0^{T_p} \phi_d(\tau) Q \phi_d(\tau)^T \, d\tau \right] \eta_d + 2\eta_d^T \left[\int_0^{T_p} \phi_d(\tau) Q e^{A\tau} \, d\tau \right] x(t_i) + 2\eta^T \Gamma \eta_d ,$$

$$(26)$$

where:

$$\Omega = \int_0^{T_p} \phi(\tau) Q \phi(\tau)^T \, d\tau + R_L,$$

$$\Psi = \int_0^{T_p} \phi(\tau) Q e^{A\tau} \, d\tau,$$

$$\Gamma = \int_0^{T_p} \phi(\tau) Q \phi_d(\tau)^T \, d\tau.$$

For the non-zero set point signal, the last element of the state vector $x(t_i)$ is given as: $y(t_i) - r(t_i)$.

From the necessary condition of the minimum P we have:

$$\frac{dP}{d\eta} = 2\Omega \eta + 2\Psi x(t_i) + 2\Gamma \eta_d = 0, \tag{27}$$

and the optimal vector of parameters η has the form:

$$\eta = -\Omega^{-1} \Psi x(t_i) - \Omega^{-1} \Gamma \eta_d. \tag{28}$$

Note that the optimal vector of parameters η for the general case is shifted by the term dependent on the measured disturbance signal. The vector of parameters

$\boldsymbol{\eta}_{\mathrm{d}}$ should be selected appropriately to minimize the performance index P in the whole optimization interval $[0, T_{\mathrm{p}}]$. The assumption that the disturbance is constant inside the given interval is valid in case of slowly changing signals. The compensator can be successfully used for the described case because the measured disturbance (temperature in the preceding zone) does not change quickly and may be known in advance due to a transport delay.

The applied parameters for predictive controller are presented in Table 2. Their values were selected arbitrarily on the basis of performed experiments.

Table 2: Parameters of the predictive controller

Parameter	Value
N	5
p	0.6
T_{p}	75

4.2. Constraints on control signals

Consideration of constraints is an essential element of each practical predictive control application. In the above subsection, the optimal control signal value is calculated regardless of constraints. However, their consideration is necessary for real control systems. In this paper only constraints for input variables are considered.

The first of them refers to the control signal amplitude. It should be limited by $u_{\min}$ and $u_{\max}$ values:

$$u_{\min} \leqslant u(t) \leqslant u_{\max}. \tag{29}$$

At the time t_i the formula:

$$u(t_i) = u(t_i - \Delta t) + \dot{u}(t_i)\Delta t = u(t_i - \Delta t) + \boldsymbol{L}(0)^T \boldsymbol{\eta}\Delta t, \tag{30}$$

where Δt is the sampling interval, is valid. Equation (30) can be derived from the definition of derivative. For the next time moments, the control signal can be written as:

$$u(\tau_i) = u(t_i) + \int_0^{\tau_i} \dot{u}(\gamma)\mathrm{d}\gamma = u(t_i) + \int_0^{\tau_i} \boldsymbol{L}(\gamma)^T \boldsymbol{\eta}\mathrm{d}\gamma$$

$$= u(t_i) + \left(\boldsymbol{L}(\tau_i)^T - \boldsymbol{L}(0)^T\right) \boldsymbol{A}_p^{-T} \boldsymbol{\eta}. \tag{31}$$

After substituting Equation (30) into Inequality (29), it has the form:

$$u_{\min} - u(t_i - \Delta t) \leqslant \boldsymbol{L}(0)^T \boldsymbol{\eta}\Delta t \leqslant u_{\max} - u(t_i - \Delta t). \tag{32}$$

Equation (32) can also be written as:

$$u_{\min} - u(t_i - \Delta t) \leqslant C_u \eta \leqslant u_{\max} - u(t_i - \Delta t), \tag{33}$$

where, from Equation (31):

$$C_u = L(0)^T \Delta t + L(\tau_i)^T A_p^{-T} - L(0)^T A_p^{-T}.$$

The second type of constraints, refers to the control signal derivatives:

$$du_{\min} \leqslant \dot{u}(t) \leqslant du_{\max}. \tag{34}$$

The suitable inequalities:

$$\begin{aligned} -L(\tau_i)^T \eta &\leqslant -du_{\min}, \\ L(\tau_i)^T \eta &\leqslant du_{\max}, \end{aligned} \tag{35}$$

are given straightforward, which results from the specificity of the algorithm.

Both types of constraints can be combined and the task can be now presented as a quadratic programming problem:

$$\begin{aligned} P &= \eta^T \Omega \eta + 2\eta^T \Psi x(t_i) + 2\eta^T \Gamma \eta_d, \\ M\eta &\leqslant \gamma, \end{aligned} \tag{36}$$

where:

$$M = \begin{bmatrix} -C_u \\ C_u \\ -L(\tau_i)^T \\ L(\tau_i)^T \end{bmatrix}, \qquad \gamma = \begin{bmatrix} -u_{\min} + u(t_i - \Delta t) \\ u_{\max} - u(t_i - \Delta t) \\ -du_{\min} \\ du_{\max} \end{bmatrix}.$$

In [17] an original approach of dealing with input constraints is proposed. This idea is also adopted during the performed experiments. When the control signal is calculated, for each numerical step while calculating $u(t)$, it is checked if any of the constraints is violated. If so, the optimal solution (without constraints) is shifted by the additional term not to exceed the limits of control signals' or their derivatives' values:

$$\begin{aligned} \lambda_{\text{act}} &= -\left(M_{\text{act}} \Omega^{-1} M_{\text{act}}^T\right)^{-1} \left(\gamma_{\text{act}} + M_{\text{act}} \left(\Omega^{-1} \Psi(\hat{x} - \hat{x}_{\text{SP}}) + \Omega^{-1} \Gamma \eta_d\right)\right), \\ \eta &= -\Omega^{-1} \Psi(\hat{x} - \hat{x}_{\text{SP}}) - \Omega^{-1} \Gamma \eta_d - \Omega^{-1} M_{\text{act}}^T \lambda_{\text{act}}, \end{aligned} \tag{37}$$

where: γ_{act} is the column vector with 1 for the active constraints and 0 for the inactive ones, M_{act} contains the rows of M referring to the active constraints.

The signals constraints for the performed experiments are given in Table 3. It is assumed that the first control signal u_1 refers to the gas-air mixture pressure, while the second u_2 concerns the cooling valve position.

Table 3: Control signals constraints

Parameter	Value
$u_{1\ min}$	0.6 kPa
$u_{1\ max}$	6 kPa
$\Delta u_{1\ min}$	$-0.15\ \dfrac{\text{kPa}}{\text{s}}$
$\Delta u_{1\ max}$	$0.15\ \dfrac{\text{kPa}}{\text{s}}$
$u_{2\ min}$	5 %
$u_{2\ max}$	75 %
$\Delta u_{2\ min}$	$-1.5\ \dfrac{\%}{\text{s}}$
$\Delta u_{2\ max}$	$1.5\ \dfrac{\%}{\text{s}}$

4.3. Set point optimization algorithm

Decribed above model identiffcation method is ued to optimize the temperature set point values in subsequent parts of the installation. This problem is widely discussed in the literature, but usually complex non-linear models are used as in [5] and [6]. Another approach to optimize the set point values for predictive controllers is discussed in [18] and adopted in this paper. In the experiments, the algorithm is applied to the last two zones of the forehearth, where stabilization of the molten glass temperature is especially crucial. It is assumed that the temperature profile for the last fourth zone is known in advance, as well as the initial set-point temperature in the third zone, whereas its deviations should be determined to be used by the optimization procedure.

The formula for a steady-state system output depending on its inputs is derived using the identified linear models. The performance index Q, defined as a squared difference between the temperature set-point and the predicted steady-state temperature for the last forehearth zone, is minimized by the set point optimization algorithm:

$$\min_{\Delta y^{\text{pr}}, u^{\text{ss}}} Q = \frac{1}{2}\left(y^{\text{sp}} - \begin{bmatrix} K_{\text{y}} & K_{\text{u}} \end{bmatrix} \begin{bmatrix} y^{\text{pr}} + \Delta y^{\text{pr}} \\ u^{\text{ss}} \end{bmatrix}\right)^2, \tag{38}$$

where: K_y – gain for the temperature in the preceding zone of the forehearth, $\boldsymbol{K}_u$ – gain for the controlled inputs of the forehearth, y^{sp} – temperature set point in the controlled zone of the forehearth, y^{pr} – temperature set point in the preceding zone of the forehearth, Δy^{pr} – temperature set point increment in the preceding zone of the forehearth, u^{ss} – control signal values in the controlled zone of the forehearth.

The set point increments and control signal values are limited by the predefined constraints:

$$
\begin{aligned}
\Delta y^{pr}_{min} &\leqslant \Delta y^{pr} \leqslant \Delta y^{pr}_{max}, \\
u^{ss}_{min} &\leqslant u^{ss} \leqslant u^{ss}_{max},
\end{aligned}
\tag{39}
$$

where: Δy^{pr}_{min}, Δy^{pr}_{max} – temperature set point increment limits for the preceding zone of the forehearth, u^{ss}_{min}, u^{ss}_{max} – limits for the steady state control signals values. Note that mentioned variables are dependent on the current operating point for the fixed control signal value u_0.

The gains values are calculated based on the identified model of the last foreherth zone as:

$$
K_y = \frac{b_{10}}{a_0}, \qquad \boldsymbol{K}_u = \left[\frac{b_{20}}{a_0} \; \ldots \; \frac{b_{K0}}{a_0} \right].
\tag{40}
$$

The parameters for performed experiments are given in Table 4. In the described case, for the last forehearth zone, the control signal u^{ss} concerns only the gas-air mixture pressure.

Table 4: Parameters of the set point optimization algorithm

Parameter	Value
Δy^{pr}_{min}	$-10°C$
Δy^{pr}_{max}	$10°C$
$u^{ss}_{min} + u_0$	1.6 kPa
$u^{ss}_{max} + u_0$	4 kPa

5. Simulation experiments

The algorithms presented above were tested using the simulation model composed of two forehearth zones. Obtained results are given in the further part of this section.

5.1. PDE model of the forehearth

The forehearth zone dynamics was simulated with the Partial Differential Equation (PDE) model. This approach is discussed in [3] and [4].

For the last fourth zone of the forehearth, the model has the following form:

$$\frac{\delta T(x,t)}{\delta t} - v(t)\frac{\delta T(x,t)}{\delta x} + K_1 T(x,t) = K_2 u_1(t), \qquad (41)$$

where: T is the molten glass temperature distribution along the zone, v is the glass velocity (it depends proportionally on the glass pull rate), u_1 is the control signal (gas-air mixture pressure). It is assumed that its influence is the same along the whole forehearth. The constant values K_1 and K_2 were identified based on the historical process data. The first of them can be interpreted as an inverse of the process time constant, while the second as the control signal gain. Their values are presented in Table 5. The boundary condition reflects the influence of the temperature in the preceding zone $w(t)$ on the simulated one:

$$T(0,t) = w(t). \qquad (42)$$

Table 5: Identfied parameters of the PDE model for the forehearth zone with a single control signal

Parameter	Value
K_1	$3.3224 \cdot 10^{-5}$
K_2	$8.7945 \cdot 10^{-3}$

For the third zone, where the cooling valve position can be additionally adjusted, a modified equation was applied:

$$\begin{aligned}
\frac{\delta T(x,t)}{\delta t} - v(t)\frac{\delta T(x,t)}{\delta x} \\
+ K_1 \left(K_3 u_2(t)^2 + K_4 u_2(t) + 1 \right) T(x,t) = K_2 u_1(t),
\end{aligned} \qquad (43)$$

where the additional parameter u_2 denotes the cooling valve position. The constant values K_3 and K_4 were identified based on the historical data as well. It was assumed that the cooling time decreases with the square of u_2 and experimental results confirmed the validity of this simplification. The boundary condition for the temperature is analogous as in the previous case. The identified parameters values are given in Table 6. The values in Tables 5 and 6 were determined based on the historical process data using the numerical optimization procedure.

Table 6: Identfied parameters of the PDE model for the forehearth zone with two control signals

Parameter	Value
K_1	$2.7935 \cdot 10^{-5}$
K_2	$1.1686 \cdot 10^{-2}$
K_3	$6.7271 \cdot 10^{-5}$
K_4	$-6.5094 \cdot 10^{-4}$

5.2. Simulation examples

Two simulation experiments are depicted in the paper. They were performed using MATLAB. PDE equations were solved with FEA Tool Multiphysics [19]. Two scenarios, typical for the real process, are presented. In the first case, the glass temperature increases, while in the second it decreases.

Before presenting the obtained results, a short description concerning the identification and control procedures is given. The identification method is intended to be performed on-line, when the successive historical data become available. Time ranges for subsequent models (that can have different structure and operating points) are denoted with different background colors. The intervals with the current model's parameters update are marked as R. The first n_{start} intervals, when the system model is not yet available are denoted with green background color.

Model predictive controller is applied from the moment when the system model is available. Up to this time, the auxiliary PID controller is used. It is also possible that the current model does not contain one of the real process inputs because it was impossible to identify this input-output dependency. Thus, this input is controlled by the PID controller. The same situation occurs when the defined control signal is inactive during the current task e.g. cooling damper position is set to its minimal value while the temperature increases. This approach is implemented to omit numerical problems when calculating the control signal in such case. In both cases (PID and MPC controllers) the sampling interval Δt is set to 10 seconds.

5.2.1. Simulation example 1

Figure 2 presents the glass pull rate changes during the experiment. The glass velocity varies from $3,128$ to $3,782$ $\frac{\text{mm}}{\text{s}}$. The real value of the parameter is marked blue and the value known for the identification algorithm is marked red. Figures 3 and 5 present the system inputs during the simulation for the third and the fourth zone respectively. The type of a utilized controller is marked with
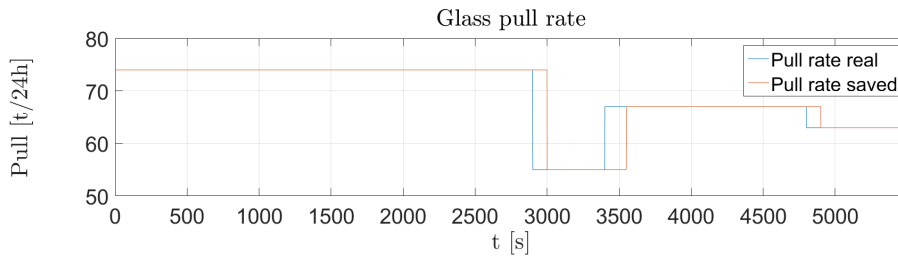
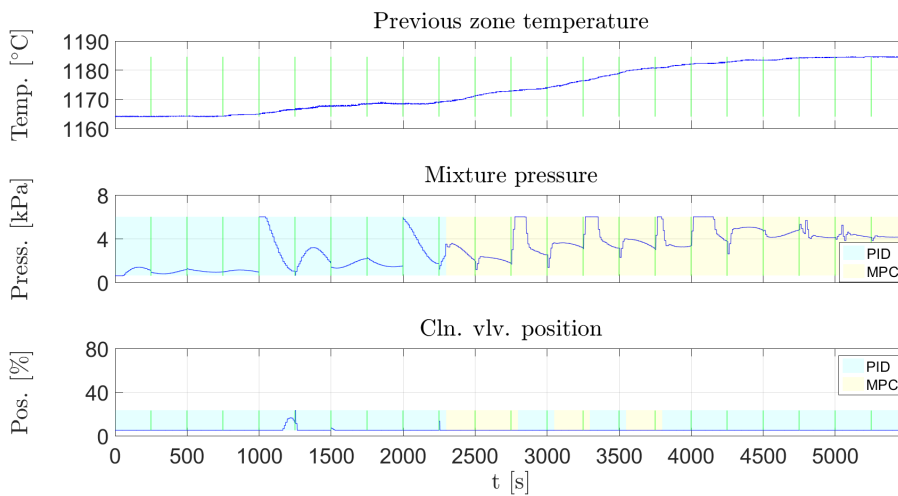Figure 2: Glass pull rate changes during the first experiment

Figure 3: Control system inputs in the third zone of the forehearth – the first experiment
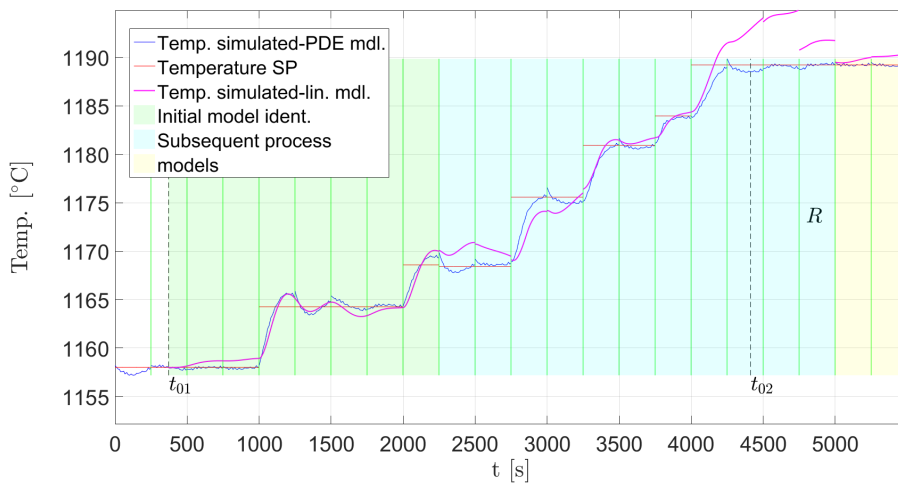

Figure 4: Simulated temperature in the third zone of the forehearth – the first experiment
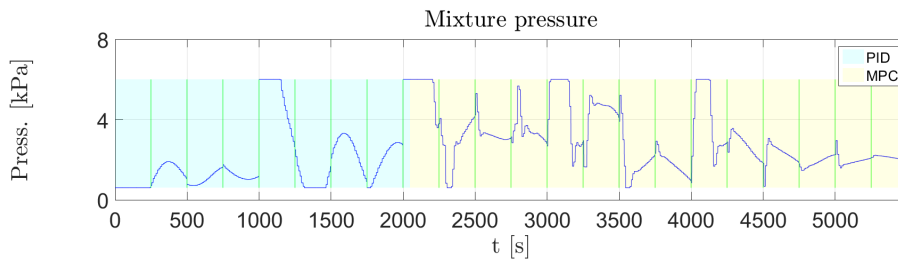
Figure 5: Control system inputs in the fourth zone of the forehearth – the first experiment
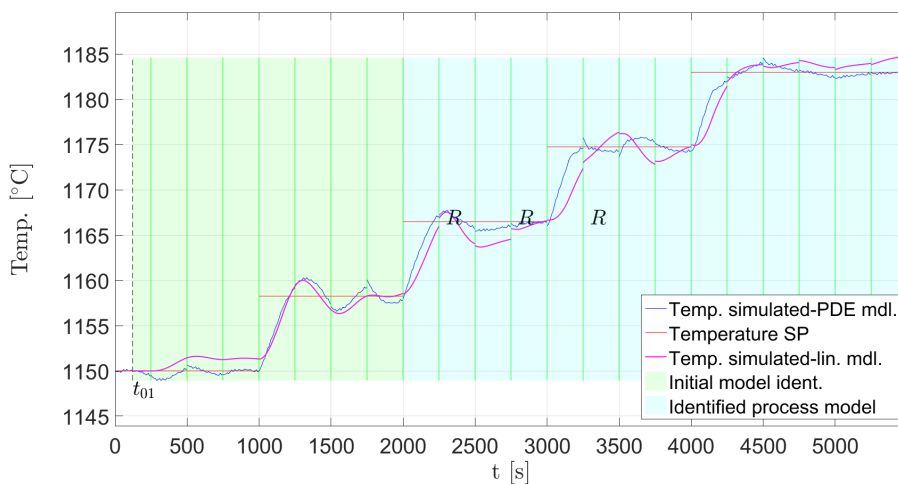

Figure 6: Simulated temperature in the fourth zone of the forehearth – the first experiment

Table 7: Identified model parameters for the third zone of the forehearth – the first experiment

Parameter	Time [s]		
	372–4750	4750–5000	5000–5500
model no	1	1	2
op. point	t_{01}	t_{01}	t_{02}
N, M	5, 6	5, 6	3, 4
h	200	200	150
a_0	$7.90 \cdot 10^{-5}$	$4.18 \cdot 10^{-5}$	$1.08 \cdot 10^{-4}$
a_1	$1.83 \cdot 10^{-2}$	$8.92 \cdot 10^{-3}$	$4.36 \cdot 10^{-3}$
a_2	1	1	1
b_{10}	$1.01 \cdot 10^{-4}$	$3.68 \cdot 10^{-5}$	$8.72 \cdot 10^{-5}$
b_{20}	$2.95 \cdot 10^{-4}$	$1.86 \cdot 10^{-4}$	$1.12 \cdot 10^{-4}$
b_{30}	$-3.77 \cdot 10^{-6}$	$-28.2 \cdot 10^{-6}$	–

a different background color. Figures 4 and 6 depict the obtained simulation results for both zones. The identified model parameters, together with the MFM properties used for their identification are given in Tables 7 and 8.

Table 8: Identified model parameters for the fourth zone of the forehearth – the first experiment

Parameter	Time [s]			
	121–2250	2250–2750	2750–3250	3250–5500
model no	1	1	1	1
op. point	t_{01}	t_{01}	t_{01}	t_{01}
N, M	3, 4	3, 4	3, 4	3, 4
h	150	150	150	150
a_0	$4.96 \cdot 10^{-5}$	$5.78 \cdot 10^{-5}$	$5.07 \cdot 10^{-5}$	$4.94 \cdot 10^{-5}$
a_1	$6.61 \cdot 10^{-3}$	$4.13 \cdot 10^{-3}$	$4.11 \cdot 10^{-3}$	$4.93 \cdot 10^{-3}$
a_2	1	1	1	1
b_{10}	$3.96 \cdot 10^{-5}$	$5.75 \cdot 10^{-5}$	$5.33 \cdot 10^{-5}$	$4.91 \cdot 10^{-5}$
b_{20}	$1.20 \cdot 10^{-4}$	$1.08 \cdot 10^{-4}$	$9.66 \cdot 10^{-5}$	$1.08 \cdot 10^{-4}$

5.2.2. Simulation example 2

In the second experiment, the glass pull rate changes as Figure 7 presents. In this case, the divergence between the real and the known pull signal value is included as well. The glass velocity varies from $3,524$ to $3,981$ $\frac{\text{mm}}{\text{s}}$. Input signals are depicted as previously in Figures 8 and 10, and the results are presented in Figures 9 and 11. The identified model parameters are gathered in Tables 9 and 10.
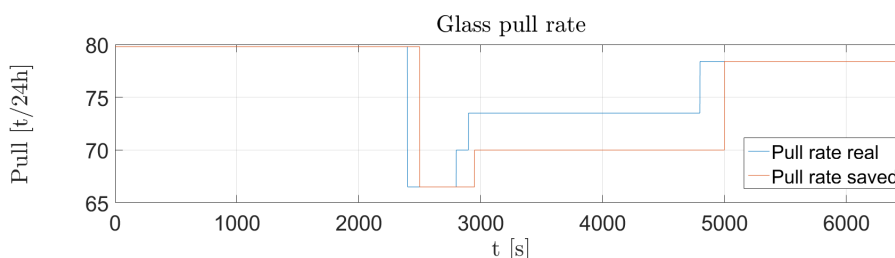

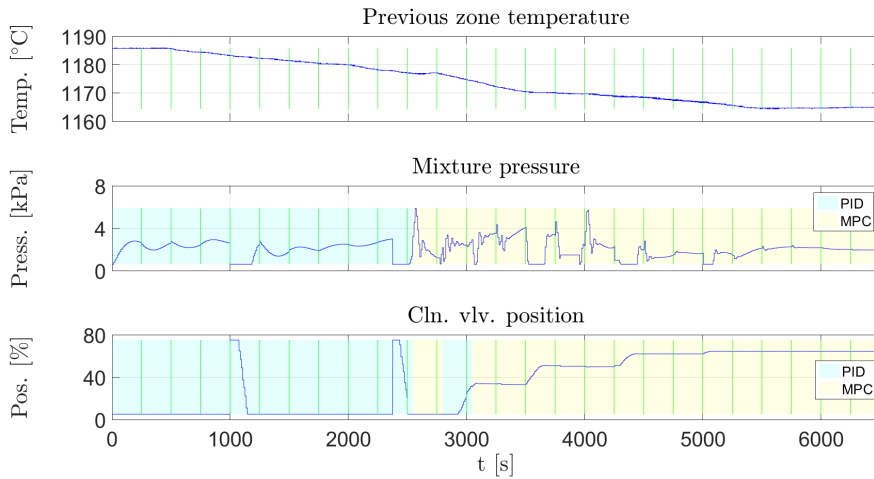Figure 7: Glass pull rate changes during the second experiment

Figure 8: Control system inputs in the third zone of the forehearth – the second experiment
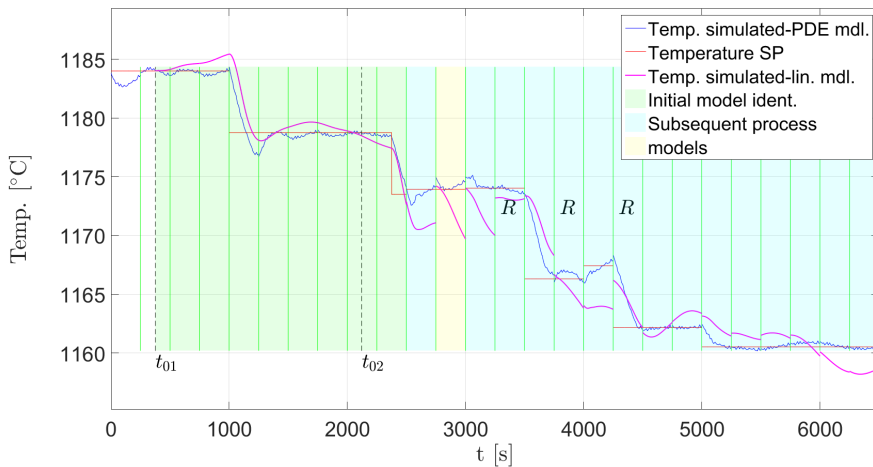

Figure 9: Simulated temperature in the third zone of the forehearth – the second experiment
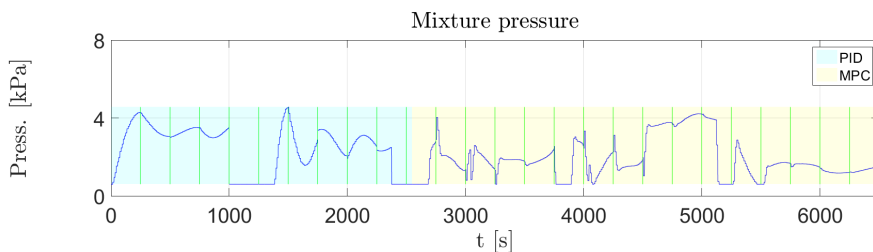

Figure 10: Control system inputs in the fourth zone of the forehearth – the second experiment

Table 9: Identified model parameters for the third zone of the forehearth – the second experiment

Parameter	Time [s]		
	376–2750	2750–3000	3000–3250
model no	1	2	3
op. point	t_{01}	t_{02}	t_{02}
N, M	5, 6	5, 6	3, 4
h	200	200	150
a_0	$4.17 \cdot 10^{-5}$	$9.49 \cdot 10^{-5}$	$7.76 \cdot 10^{-5}$
a_1	$1.16 \cdot 10^{-2}$	$1.79 \cdot 10^{-2}$	$1.47 \cdot 10^{-2}$
a_2	1	1	1
b_{10}	$7.27 \cdot 10^{-5}$	$2.15 \cdot 10^{-4}$	$1.12 \cdot 10^{-4}$
b_{20}	$1.03 \cdot 10^{-4}$	$5.74 \cdot 10^{-5}$	$9.11 \cdot 10^{-5}$
b_{30}	$-1.07 \cdot 10^{-5}$	–	$-1.11 \cdot 10^{-5}$
Parameter	Time [s]		
	3250–3750	3750–4250	4250–6500
model no	3	3	3
op. point	t_{02}	t_{02}	t_{02}
N, M	3, 4	3, 4	3, 4
h	150	150	150
a_0	$5.32 \cdot 10^{-5}$	$8.14 \cdot 10^{-5}$	$7.55 \cdot 10^{-5}$
a_1	$1.40 \cdot 10^{-2}$	$8.19 \cdot 10^{-3}$	$4.42 \cdot 10^{-3}$
a_2	1	1	1
b_{10}	$4.12 \cdot 10^{-5}$	$9.45 \cdot 10^{-5}$	$7.45 \cdot 10^{-5}$
b_{20}	$1.50 \cdot 10^{-4}$	$1.30 \cdot 10^{-4}$	$9.89 \cdot 10^{-5}$
b_{30}	$-8.12 \cdot 10^{-6}$	$-4.34 \cdot 10^{-6}$	$-3.52 \cdot 10^{-6}$

Table 10: Identified model parameters for the fourth zone of the forehearth – the second experiment

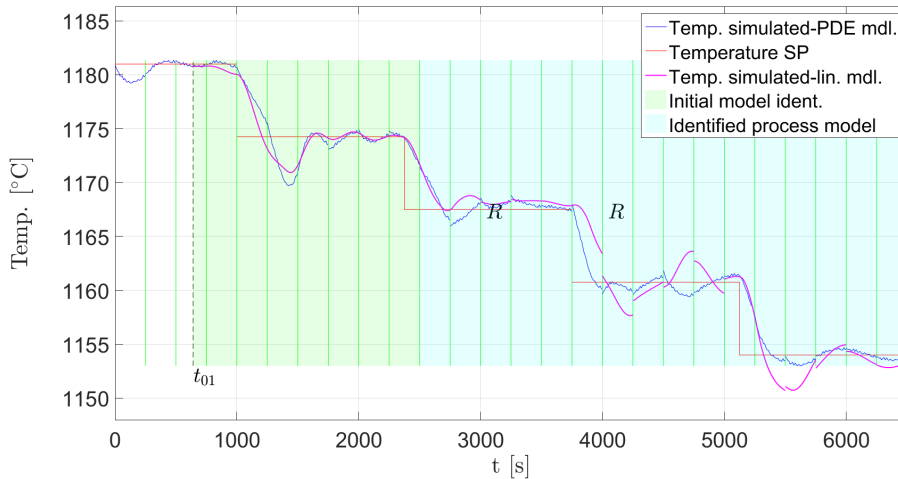| Parameter	Time [s]		
	640–3000	3000–4000	4000–6500
model no	1	1	1
op. point	t_{01}	t_{01}	t_{01}
N, M	3, 4	3, 4	3, 4
h	200	200	200
a_0	$8.09 \cdot 10^{-5}$	$6.89 \cdot 10^{-5}$	$7.96 \cdot 10^{-5}$
a_1	$6.44 \cdot 10^{-3}$	$5.28 \cdot 10^{-3}$	$3.36 \cdot 10^{-3}$
a_2	1	1	1
b_{10}	$7.13 \cdot 10^{-5}$	$6.03 \cdot 10^{-5}$	$7.77 \cdot 10^{-5}$
b_{20}	$1.98 \cdot 10^{-4}$	$1.75 \cdot 10^{-4}$	$1.71 \cdot 10^{-4}$

Figure 11: Simulated temperature in the fourth zone of the forehearth – the second experiment

6. Conclusion

Comprehensive approach to the problem of process model identification and control of the glass conditioning process is described in the paper. The presented simulation results proved that the method can be successfully implemented for the task. The mean squared differences between the simulated process outputs and the desired set point values are given in Table 11. The obtained results are repetitive, which proves the method robustness.

Table 11: Mean squared difference between the temperature set point and the simulated value

Experiment no	Zone no	
	3	4
1	1.7857	3.8804
2	1.5448	3.2414

The algorithm enables control of the separate control loops for both zones of the forehearth more accurately, as well as it makes steady state optimization possible which keeps the desired temperature profile in the most important last part of the installation. The described approach could be applied to a real industrial plant without major changes.

References

[1] Q. WANG, Q. CHALAYE, G. THOMAS, and G. GILLES: Predictive control of a glass process. *Control Engineering Practice*, **5**(2), (1997), 167–173. DOI: 10.1016/S0967-0661(97)00223-2.

[2] B. GOUGH, J. KAY, and G. DUMONT: Advanced model based control for continuous process industries. In: *Proceedings of the 1997 American Control Conference (Cat. No.97CH36041)*, (1997), 579–584. DOI: 10.1109/ACC.1997.611865.

[3] A. KHARITONOV, S. HENKEL, and O. SAWODNY: Two degree of freedom control for a glass feeder. In: *Proceedings of the European Control Conference*, (2007), 4079–4086. DOI: 10.23919/ECC.2007.7068450.

[4] S. HENKEL, A. KHARITONOV, and O. SAWODNY: Modelling and optimisation of a glass feeder considered as a distributed parameter system. *SICE Annual Conference*, (2007), 2950–2954. DOI: 10.1109/SICE.2007.4421496.

[5] E. MUYSENBERG, J. CHMELAR, R. BODI, and F. MATUSIK: Practical examples and advantages of advanced control applications by expert system ESII. In: *A collection of papers presented at the 62nd Conference on Glass Problems*, (2002), 3–19. DOI: 10.1002/9780470294727.ch1.

[6] E. MUYSENBERG, G. NEFF, J. MULLER, J. CHMELAR, R. BODI, and F. MATUSIK: An advanced control system to increase glass quality and glass production yields based on GS ESIII technology. In: *A Collection of Papers Presented at the 66th Conference on Glass Problems*, (2005), 33–45. DOI: 10.1002/9780470291306.ch3.

[7] W. BYRSKI, M. DRAPAŁA, and J. BYRSKI: An adaptive identification method based on the modulating functions technique and exact state observers for modeling and simulation of a nonlinear MISO glass melting process. *International Journal of Applied Mathematics and Computer Science*, **29**(4), (2019), 739–757. DOI: 10.2478/amcs-2019-0055.

[8] W. BYRSKI, M. DRAPAŁA, and J. BYRSKI: New on-line algorithms for modelling, identification and simulation of dynamic systems using modulating functions and non-asymptotic state estimators: Case study for a chosen physical process. *International Conference of Computer Science 2021*, (2021), 284–297. DOI: 10.1007/978-3-030-77970-2_22.

[9] M. DRAPAŁA and W. BYRSKI: Continuous-time model predictive control with disturbances compensation for a glass forehearth. *25th International Conference on Methods and Models in Automation and Robotics (MMAR)*, (2021), 366–371. DOI: 10.1109/MMAR49549.2021.9528433.

[10] M. SHINBROT: On the analysis of linear and nonlinear systems. *Transactions of the American Society of Mechanical Engineers: Journal of Basic Engineering*, **79**(3), (1957), 547–522. DOI: 10.1115/1.4013092.

[11] W. BYRSKI and S. FUKSA: Optimal identification of continuous systems in L_2 space by the use of compact support filter. *International Journal of Modelling and Simulation*, **15**(4), (1995), 125–131. DOI: 10.1080/02286203.1995.11760263.

[12] W. BYRSKI and J. BYRSKI: The role of parameter constraints in EE and OE methods for optimal identification of continuous LTI models. *International Journal of Applied Mathematics and Computer Science*, **22**(2), (2012), 379–388. DOI: 10.2478/v10006-012-0028-3.

[13] W. BYRSKI: The survey for the exact and optimal state observers in Hilbert spaces. *2003 European Control Conference (ECC)*, (2003), 3548–3553. DOI: 10.23919/ECC.2003.7086592.

[14] P. AIRIKKA: Advanced control methods for industrial process control. *Computing and Control Engineering Journal*, **15**(3), (2004), 18–23. DOI: 10.1049/cce:20040303.

[15] S.J. QIN and T.A. BADGWELL: A survey of industrial model predictive control technology. *Control Engineering Practice*, **11**(7), (2004), 733–764. DOI: 10.1016/S0967-0661(02)00186-7.

[16] M. MORARI and H.L. JAY: Model predictive control: past, present and future. *Computers & Chemical Engineering*, **23**(4), (1999), 667–682. DOI: 10.1016/S0098-1354(98)00301-9.

[17] L. WANG: *Model Predictive Control System Design and Implementation using MATLAB®*. Springer, London, 2009.

[18] P. TATJEWSKI: *Advanced Control of Industrial Processes: Structures and Algorithms*. Springer, London, 2007.

[19] PRECISE SIMULATION LTD., HONG KONG: FEATool Multiphysics v 1.11 User's Guide: https://www.featool.com [Access date: 04.01.2022].